

We are IntechOpen, the world's leading publisher of Open Access books Built by scientists, for scientists

6,400

Open access books available

174,000

International authors and editors

190M

Downloads

Our authors are among the

154

Countries delivered to

TOP 1%

most cited scientists

12.2%

Contributors from top 500 universities



WEB OF SCIENCE™

Selection of our books indexed in the Book Citation Index
in Web of Science™ Core Collection (BKCI)

Interested in publishing with us?
Contact book.department@intechopen.com

Numbers displayed above are based on latest data collected.
For more information visit www.intechopen.com



Chapter

Anatomy-Based Programming

Isra Aljazeera, Yassin Abdelsamad and Abdulrahman Hagr

Abstract

The ultimate goal of a cochlear implant device is to mimic the hearing through normal cochlea. A better understanding of normal cochlear function can help reaching this goal. The normal cochlea has a tonotopic mapping of the frequency representation in which each area on the cochlea is the most sensitive to a specific frequency. The array of the cochlear implant device has a number of electrodes each presenting a different frequency to the nearest area of the cochlea to where they are located. An anatomy-based programming strategy aims to present the frequency by the electrode contacts to which the cochlea is most sensitive to, according to the location of that electrode contact inside the cochlea. This chapter explores the details of the current understanding of the anatomy-based programming.

Keywords: cochlea, anatomy, anatomy-based, programming, fitting, frequency-to-place mismatch

1. Introduction

Cochlear implant device is one of the most successful invented implants. It is used in patients who have lost their hearing sensation and have sensorineural hearing loss. The cochlear implant device has an external part containing a microphone and speech processor and an internal part that is implanted surgically and contains an internal receiver stimulator and an electrode array. The internal part of the multichannel cochlear implant contains a number of electrode contacts arranged along its electrode array which is inserted inside the cochlea. These electrode contacts stimulate different locations inside the cochlea to achieve a frequency-based pitch perception which helps in speech understanding. Once the patient is implanted, the audiologists start programming the device to achieve the best hearing outcome. Cochlear implant programming includes allocating specific frequencies to each electrode contact. And since the cochlear implant is aiming to replace the normal cochlear sensation, the frequency allocations are programmed in a way to simulate the exponential logarithmic function of the normal cochlea's frequency map. To have a better understanding of the concepts behind anatomy-based programming, we need to understand the relevant cochlear anatomy and physiology of pitch perception which will be discussed in this chapter. Reaching a patient-specific anatomy-based programming then includes clinical application of measuring the relevant anatomical variables that is not an easy task to perform, and we will discuss the difficulties in this process in this chapter.

2. Relevant cochlear anatomy

The cochlea is a hollow spiral structure in the inner ear that is responsible for the hearing sensation. It is contained within the petrous portion of the temporal bone. The spiral hallow of the cochlea turns around a central bony pyramid called modiolus. A thin bony plate, called the osseous spiral lamina, is connected to the modiolus and divides the bony cochlea incompletely. The cochlear lumen is divided into three spaces by two membranes that are attached to the spiral lamina; the basilar membrane that separates the scala tympani from the scala media and the Reissner's membrane that separates the scala media from the scala vestibuli. The organ of corti is supported on the basilar membrane and contains the hearing sensory cells. From the basilar membrane, nerve fibers travel to the spiral ganglion, a structure that is located closer to the cochlear spiral's axis of rotation and includes neuron cell bodies.

During cochlear implantation, an electrode array is placed in the scala tympani of the cochlea to stimulate the cochlear nerve and induce action potentials. It is still undetermined where these APs are evoked along the sensorineural pathway of the hearing (**Figure 1**) [1].

2.1 Basilar membrane

The acoustic stimulus causes the vibration of the tympanic membrane and in turn the ossicular chain, ending in the vibration of the footplate of the stapes that causes a wave in the perilymphatic fluid inside the scala vestibuli which is transferred to the basilar membrane. Von Bekesy in his Nobel Lecture, in the 1960s, was the first to introduce the

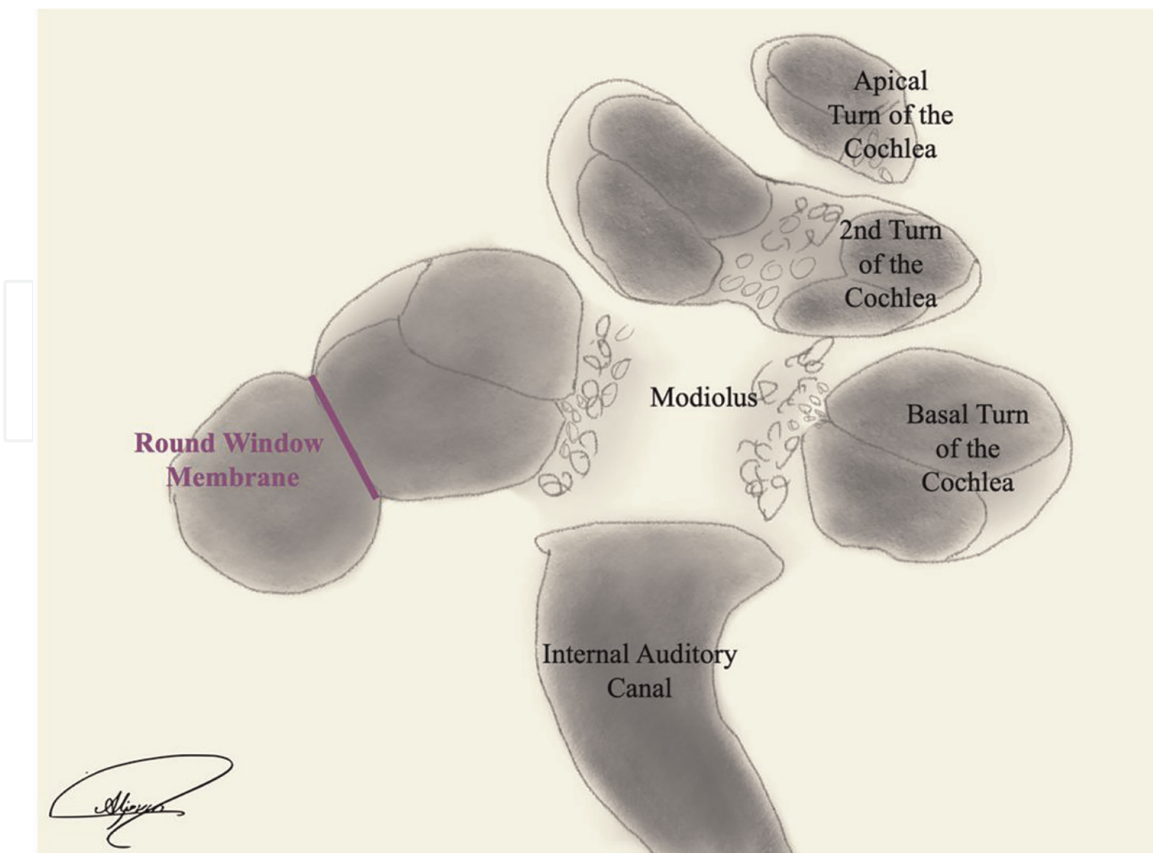


Figure 1. Showing the anatomy of the cochlea as seen in a mid-modiolar view in a micro-CT image of the temporal bone.

concept of this cochlear traveling wave along the basilar membrane. The maximum vibration amplitude of this wave along the basilar membrane is located in a different place according to the stimulus frequency, resulting in an increased sensitivity of that place in the basilar membrane to that special frequency. The frequency to which the basilar membrane shows the most sensitivity is called the characteristic frequency [2–4].

The physical properties of the basilar membrane and the cochlear fluids determine the characteristic frequencies along the basilar membrane. Although the cochlear structure maintains relatively the same along the length of the cochlea, there are three changes to its physical properties. First, the cochlear lumen decreases from the base toward the apex. Second, the basilar membrane mass is higher in the base in compared to the apex due to the increased number and size of the supporting cells. Third, the basilar membrane is stiffer by about 100-fold at the base in compared to the apex. These changes in the physical properties of the basilar membrane result in a change of the amplitude of the cochlear traveling wave. The wave increases in amplitude while traveling from the base toward the apex, till it reaches the place of the maximum amplitude, beyond which it declines. The place of the maximum amplitude is dependent on the characteristic frequency for that place resulting in a spatial cochlear frequency map. This spatial frequency sensitivity map is what is referred to as the cochlear tonotopicity (**Figure 2**) [5].

The characteristic frequency of each place on the cochlea can be calculated using an equation introduced by Greenwood. In this equation, the input is the vibratory length of the basilar membrane containing the sensory organ of corti [6].

The standard of preoperative evaluation of cochlear implant patients have been either computed tomography (CT), magnetic resonance imaging (MRI), or both for decades now. However, both these imaging techniques lack the spatial resolution needed to visualize the basilar membrane which is needed for the Greenwood frequency eq. [7].

Since the actual measurement of the length of the organ of corti is not feasible during the routine imaging, an estimate is made through a number of steps. The organ of corti on the basilar membrane runs closer to the lateral bony wall of the cochlea.

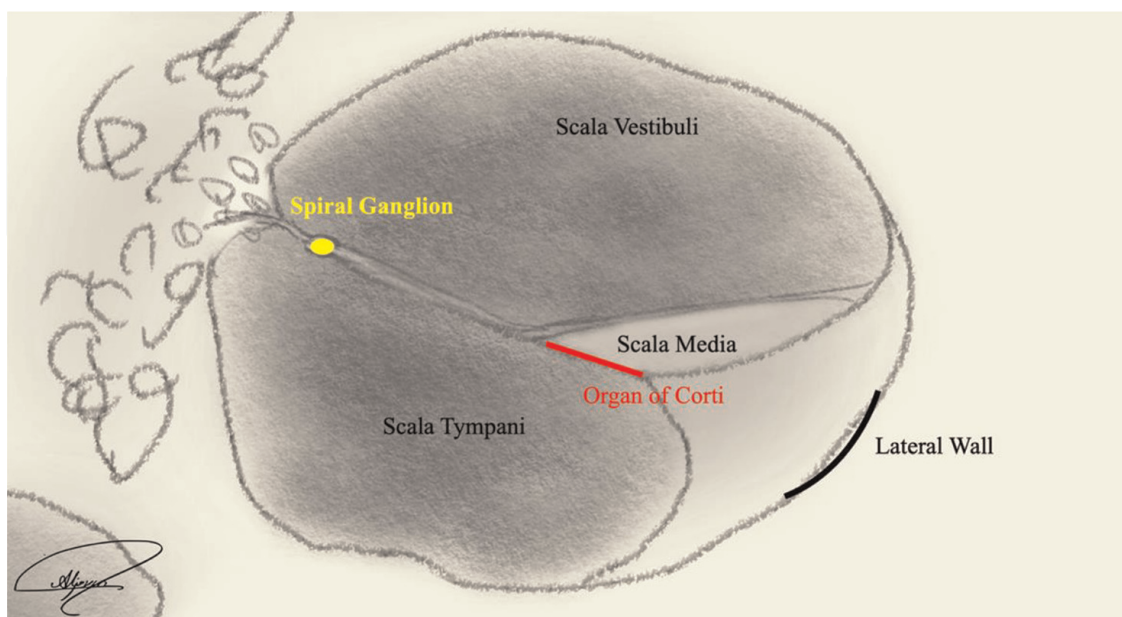


Figure 2. Illustrating the location of the spiral ganglion, the organ of corti, and the lateral wall as would be seen in a micro-CT image.

Although the lateral bony wall of the cochlea does not contain any special hearing structures, it is of utmost clinical importance. This is because it is easily observed via the routinely performed CT imaging studies that are performed for the evaluation of cochlear implantation patients. Hence, its length has been used as an estimate to the length of the basilar membrane.

2.2 Helicotrema

The helicotrema is the most apical part of the cochlea that lacks basilar membrane. It starts where the scala tympani and the scala vestibuli merge, to the apical end of the cochlear bony wall [8, 9].

An accurate measurement of the basilar membrane length is a prerequisite for anatomy-based programming calculations. The lack of visible boundaries in the end point of the cochlear apex using routine high-resolution CT resulted in an inaccurate estimation of the length of the basilar membrane. Furthermore, the total cochlear rotation is highly variable in the apex, resulting in an additional inaccuracy in the cochlear duct length (CDL) measurement modeling techniques [10–12].

Using synchrotron radiation phase-contrast imaging, the length of the basilar membrane has been found to be highly correlated to the bony cochlear duct length using the following equation:

$$\text{Basilar membrane length} = 0.88(\text{CDL}_{\text{TIP}}) + 3.71.$$

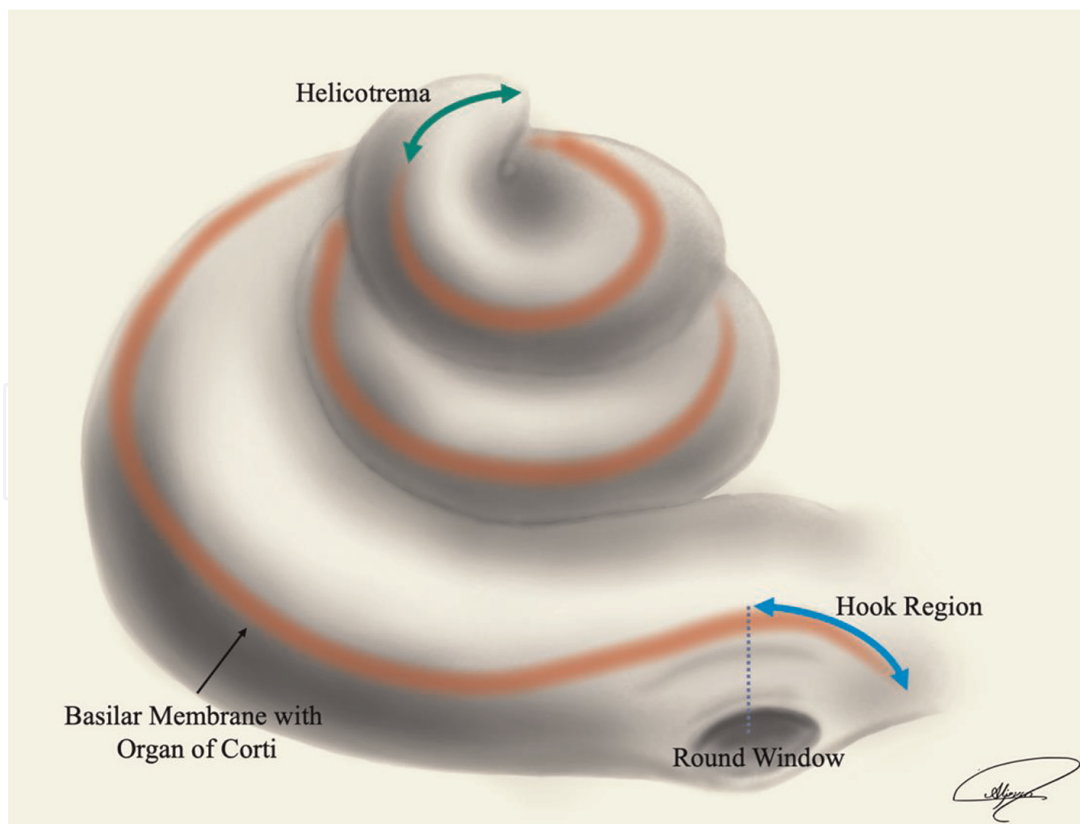


Figure 3. Illustrating the location of the hook region and the helicotrema in the cochlea. The hook region is the part of the basilar membrane starting before the midpoint of the round window which is the anatomical part that is easily seen in a high-resolution CT. The helicotrema is the part of the cochlear length that lacks basilar membrane structure.

where CDL_{TIP} refers to the length of CDL to the tip of the bony wall of the cochlea.

The use of this correction can help in a more accurate measurement of the basilar membrane [13].

2.3 Hook region

The hook region is the most basal part of the cochlear bony canal, which forms a curvature beyond the level of the round window [14, 15].

The basilar membrane continues in the hook region of the cochlea. This means that for a more accurate calculation of the place-related tonotopic representation, the length of the hook region needs to be considered and corrected. Furthermore, the connective dendrites in the hook region follow a nonradial trajectory from the basilar membrane to the spiral ganglion, which needs to be considered in evaluating the spiral ganglion tonotopic map.

Using synchrotron radiation phase-contrast imaging, an addition of a 2.5 mm as an average of the hook region length can improve the accuracy of the basilar membrane measurement (**Figure 3**) [16].

3. Mechanisms of hearing

3.1 Pitch perception

The pitch of a sound is the subjective perception of that sound on a musical scale [17]. The perception of sound pitch is believed to be determined through two functions: the spatial and temporal cues of the sound. The spatial cues of the sounds are elicited by the place where the peak of electrical stimulation is located in the tonotopic map of the cochlea.

The temporal cues are determined by the precise timing of the action potentials at a certain phase within the cycle of the sound tone, resulting in a specific time interval between the action potentials [18]. The temporal cues have been found to be more of importance in the lower frequencies, after which becoming difficult to detect experimentally, in a phenomenon called phase locking. The level of phase locking has been found to be at about 1–2 kHz depending on the species.

The electrical hearing in cochlear implanted recipients would result in a better synchronization compared to the acoustic hearing, which might suggest a more reliable pitch perception with temporal cues [19, 20].

However, in cochlear implant recipients, 300 Hz was found to be the upper boundary of temporal cue function in pitch perception. It needs to be mentioned that the inability to discriminate temporal cues does not necessarily mean that the temporal information is not processed, as the physiological psychophysical studies shown detection of temporal fluctuations as high as 4 kHz [21–23]. This upper limit can affect the ability of CI recipients to recognize melodies and musical intervals and their ability to detect minor changes in frequencies using temporal cues which is present in normal hearing cochlea till up to 4–5 kHz [24–26].

The use of functional MRI in more recent studies have been used in a try to shade more light on the understanding of pitch perception in human, specially that the invasive nature of phase lock measurement has prevented its actual measurement in human. This area however yet needs further study since no consensus has been reached on the tonotopic organization of the auditory brain areas [27–31].

4. Calculation of characteristic frequency

4.1 Calculation of characteristic frequency and anatomy-based frequency allocation

There are mainly two widely known methods to calculate the characteristic frequencies, based on the tonotopic map of the two most probable areas where the electrical stimulus first picked up along the sensorineural elements of the cochlea. First is the Greenwood's function that estimates the characteristic frequencies along the organ of corti. The second is the Stakhovskaya frequency map for the spiral ganglion [32].

Greenwood equation is a near-logarithmic function relating the frequency to the relative position of the area being studied within the whole length of the organ of corti. The equation is as follows:

$$f = 165.4 (10^{2.1x} - 0.88)$$

where f is the characteristic frequency of the area of interest and x is fractional length of the area or interest along the OC:

$$x = [CDL_{oc} - CDL_{oc}(\theta)]/CDL_{oc}$$

Measuring the length of the organ of corti, which is needed for the Greenwood equation, is still a matter of study. To estimate this length for a CI recipient, a CT image is usually used. The CT image can show the bony boundaries of the cochlea. The use of CT image for this estimation results in a number of inaccuracies. First, the OC is not exactly located in the lateral bony wall, but rather more medially. To overcome this inaccuracy, Alexiades has proposed an equation to correct for the medial position of the OC in relation to the lateral cochlear bony wall as follows:

$$CDL_{oc} = \left[1.71 * \left[1 * 1 : 18 * (A_{oc}) + 2 : 69 * (B_{oc}) - \sqrt{0.72 * A_{oc} * B_{oc}} \right] * 0 : 18 \right]$$

where value A_{oc} is corrected length of the OC for the linear measurement from the round window to the furthest lateral wall on the opposite side of the basal turn of the cochlea, and value B_{oc} is corrected length of the OC for the linear measurement perpendicular to the cochlear opposite lateral walls' diameter.

The second inaccuracy is due to the fact that the cochlear parameters used to measure the CDL use the visible anatomy of the midpoint of the round window as the start point for measurement. This start point disregards the presence of the OC in the hook region, beyond the round window. Recent sychotron imaging-based anatomical studies suggest adding a correction factor of 2.5 mm to the OC length as the mean of hook region length [16]. Although there is a variability in the cochlear height, the effect of this variability on the CDL is still poorly studied, which can be another source of inaccurate CDL estimation [33–35].

Stakhovskaya map, which is the second method to calculate the characteristic frequencies, was driven from the radial trajectory of the organ of corti Greenwood map. This map suggests a constant frequency map according to the angle of the place in the cochlea to be studied with disregard to the anatomical variations in the CDL, OC, and SG lengths. In forming of Stakhovskaya map, two-dimensional cochlear views were used that might not perfectly represent the three-dimensional reality of the cochlea. Furthermore, the relation of the OC and SG does not continue as perfect radial trajectories since the length of the OC continues beyond the level where the SG

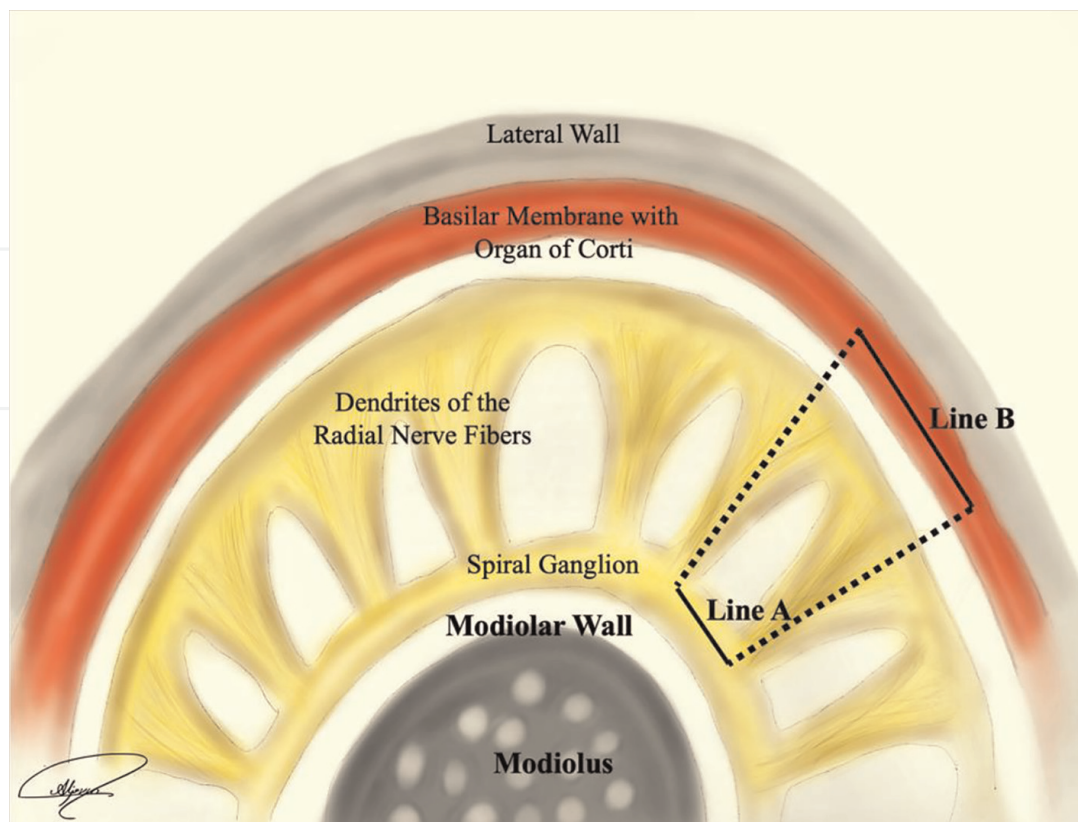


Figure 4. Stakhovskaya calculated the spiral ganglion tonotopicity map as a function of basilar membrane tonotopicity map, by correlating the length of line A, representing the spiral ganglion length, in relation to line B, representing the basilar membrane length.

length ends, making the more apical areas of the SG highly condensed with OC representing dendrites (**Figure 4**).

Using the 3D synchrotron radiation phase-contrast imaging, the spiral ganglion angle-frequency function can be calculated using the following equation:

$$f = 2^{(-0.12\theta + 160/12)}$$

where θ stands for the angular depth, measured from the center of the RW.

These measures were not observed to significantly differ from that of Stakhovskaya frequency map [36]. The spiral ganglion tonotopicity is highly compacted at its apex, which makes it extremely difficult to selectively excite low-frequency neurons.

4.2 Calculation of the frequency-to-place mismatch

The amount of the frequency-to-place mismatch is calculated by determining the difference in the frequency presented by each electrode contact and the characteristic frequency of the place where this electrode contact is located.

4.3 Determinants of frequency-to-place mismatch

Frequency-to-place mismatch happens when the electrode presents a frequency stimulus to a place in the cochlea that does not match the frequency to which that place shows the highest sensitivity to.

This discrepancy is due to the relative misplacement of two places with same frequency to each other, namely the place of the electrode contact that is programmed to stimulate a specific frequency and the place in the cochlea with that same characteristic frequency.

After surgical placing of the electrode contact, the place of the electrode contact is determined and to match the frequency-to-place, the fitting of the electrode contact can be changed to adjust to the characteristic frequency of the cochlea where the contact is located.

Using a default frequency map for all patients has shown to result in a significant mismatch.

The first determinant of the mismatch is the length of the electrode. The current electrode designs have different active stimulating ranges in which the contacts are located. The Greenwood equation takes into consideration the location of the electrode contacts to calculate the characteristic frequency of that place. Given the same default map for all designs, the different lengths of the electrode arrays result in different insertion depth with full insertion, and therefore in different characteristic frequencies they face, which in turn results in different extent of mismatch (**Figure 5**) [37].

The second determinant of the mismatch is the cochlear duct length, which is the other variable in the Greenwood equation. There is a vast variability in the cochlear duct length in normal population that ranges from 19.71 to 45.6 mm. To add more to this complexity, there are a large number of cochlear implant recipients who have cochlear anomalies that can affect the cochlear duct length (**Figure 6**) [32, 35, 38, 39].

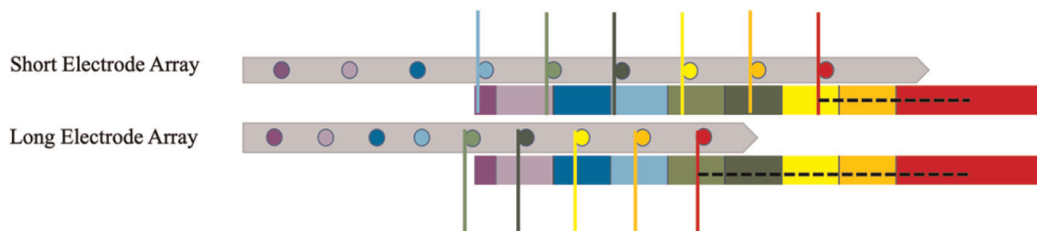


Figure 5.
The effect of the electrode length on the magnitude of the mismatch, illustrated as dashed black line, when default frequency mapping is used.

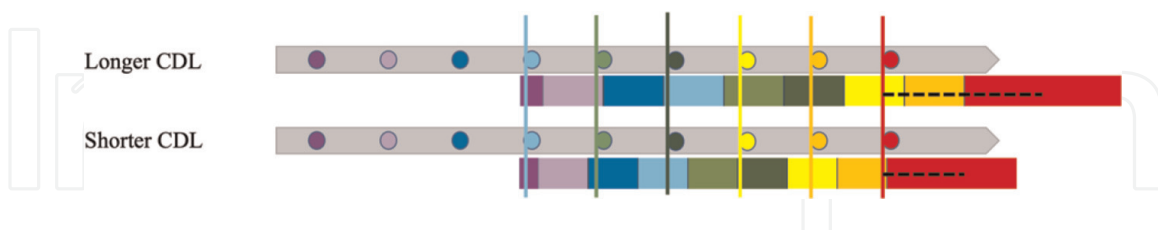


Figure 6.
The effect of the cochlear duct length (CDL) on the magnitude of the mismatch, illustrated as dashed black line, when default frequency mapping is used.



Figure 7.
The effect of the degree of insertion on the magnitude of the mismatch, illustrated as dashed black line, when default frequency mapping is used.

The last determinant is the surgical position of the electrode array according to the depth of insertion (**Figure 7**).

5. The importance of frequency-to-place mismatch

As discussed in the previous section, the impact of frequency-to-place mismatch is still under study. However, theoretically there are special scenarios where the frequency-to-place mismatch is theorized to be of more importance.

One of them is in the patients who have any sort of hearing memory, where they have had acoustic hearing that was lost afterward. This category includes a large portion of implanted patients with various etiologies that can either be a progressive hearing loss, presbycusis, sudden sensorineural hearing loss or patients who lost their hearing after temporal bone trauma or otological surgery. It is assumed that these patients would remember the characteristic frequency of each location in their cochlea and would compare the electric hearing to their memory of the acoustic hearing.



Figure 8.
The difference between default and anatomy-based map in a case of single sided deafness.

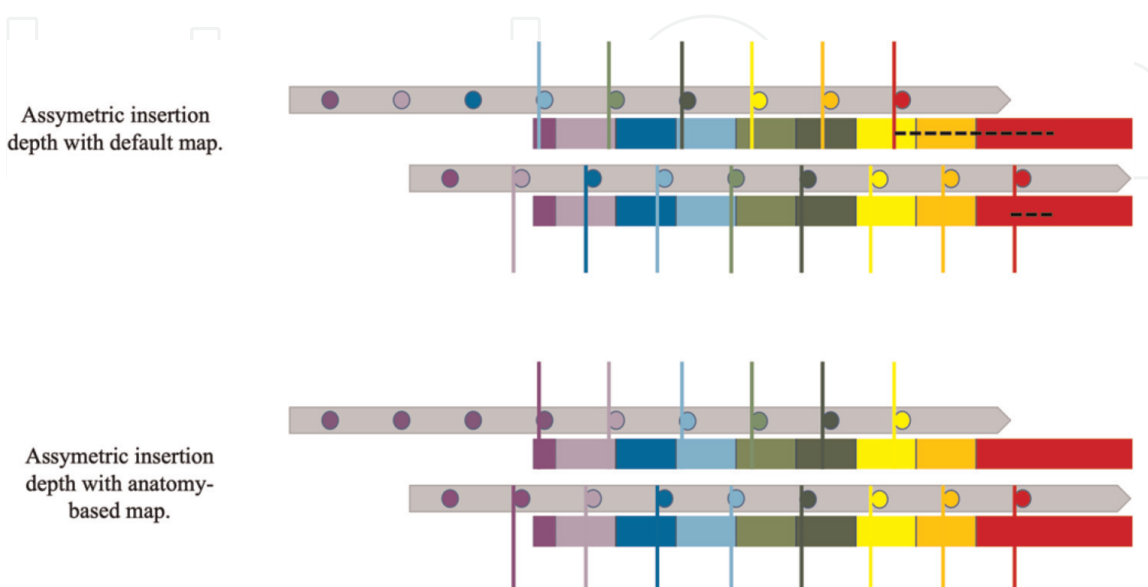


Figure 9.
The difference between default and anatomy-based map in a case with asymmetrical insertion depth.

Anatomy-based programming was found to be associated with a better auditory outcome in postlingual adults [40].

The second category are patients with single-sided hearing, even if they do not have any hearing memory in the deafened ear, and these patients could compare the hearing in the implanted ear to the hearing in the contralateral normal ear with the normal tonotopicity. And it has been shown that patients with single sided deafness (SSD) have a high rate of nonuse and not all will cope to the use of CI (**Figure 8**).

The third category are patients with bilateral CI who have different insertion depth, different electrode lengths, or different cochlear duct length in the two cochleae. Giving an anatomy-based fitting to these patients would result in a more balanced and symmetrical hearing and is theorized to have a more acceptable presentation to the brain (**Figure 9**).

6. The clinical impact of frequency-to-place mismatch

Considering the three determinants of the frequency-to-place mismatch, the effect of each of these determinants on the auditory and speech outcomes can be considered as an indirect effect of a better frequency-to-place matching.

Numerous articles have shown a better outcome with longer electrodes and deeper insertion including speech recognition scores. The studies also showed that these superior auditory outcomes appear in the early post-activation period and were sustained in long-term use [41–48]. Patients with single-sided deafness showed improved head shadow benefits as well as better spatial release of masking with a better frequency-to-place matching [49]. Better auditory outcomes have been found in association with a better frequency-to-place matching in elderly adults, which may be of particular benefit to them considering the age-related deficit in the auditory processing [40].

7. Areas to explore

There is still unclear where the site of stimulation is in the cochlea, whether it is the organ of corti, the spiral ganglion, a combination of both, or even somewhere else.

While the organ of corti continues till the level of the helicotrema in the apical turn, the spiral ganglion does not go further than half of the second turn. Argue can be made whether there is a need for a deeper cochlear insertion and longer electrodes to cover all the length of the OC or is it enough that we reach up to the level where the SG ends. And although the OC course and length is more predictable using the routine CT imaging, the SG has an unpredictable and steep and condense tonotopic presentation at its more apical end and would be extremely difficult to achieve a proper frequency-to-place matching at that area (**Figure 10**).

The other consideration for a perfect frequency-to-place matching is the fact that to achieve that, we are losing some of the low-frequency perception that is not covered with the electrode in the OC mapping specially. This area of noncoverage will be more with shorter electrodes. However, it needs to be considered that the normal hearing covers up to 20 Hz as the lower frequency limit, and the effect of covering this low level of frequency with cochlear implant is not supposed to be high in speech perception and intelligibility [50]. Future studies on the site of the first stimulus generation are needed to shade light on this matter (**Figure 11**).

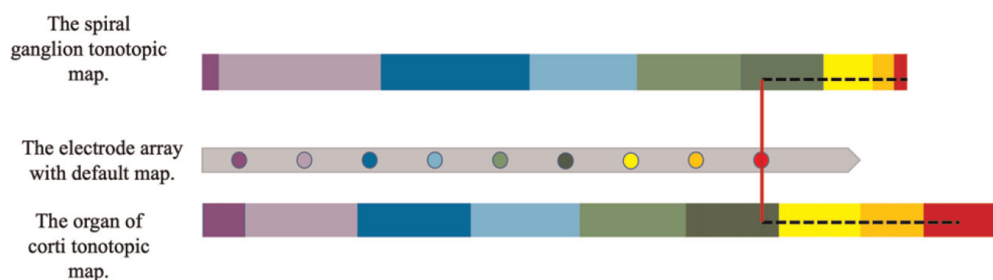


Figure 10.
The difference between the frequency-to-place mismatch using the organ of corti map in compared to the spiral ganglion map.

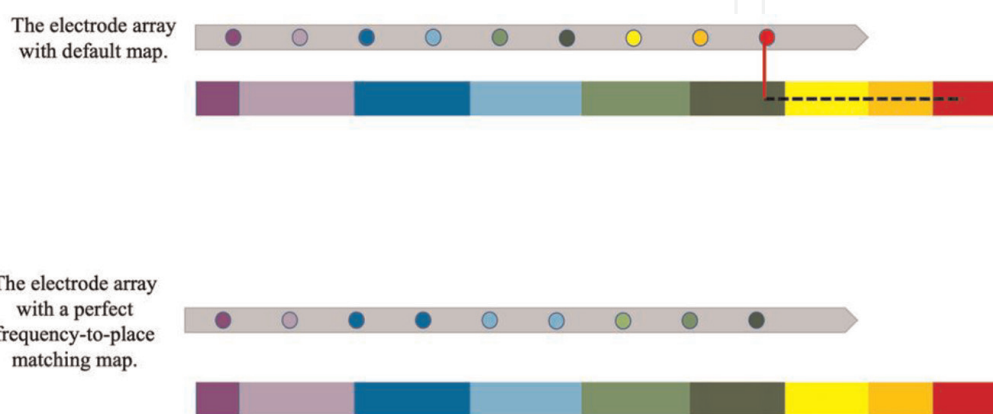


Figure 11.
The difference between default and a perfect anatomy-based map in the ability to cover the lower frequencies.

8. Conclusion

A default frequency fitting results in a wide variability of frequency-to-place mismatch. The variability of the magnitude of the frequency-to-place mismatch is dependent on the degree of insertion, length of the electrode, and the cochlear duct length. The anatomy-based fitting provides a personalized frequency map for the CI users that aim to better imitate the tonotopocity of the normal cochlea. The current evidence suggests that anatomy-based fitting can enhance the CI user benefit.

Conflict of interest

“The author declares no conflict of interest.”

IntechOpen

Author details

Isra Aljazeera^{1,2*}, Yassin Abdelsamad³ and Abdulrahman Hagr²


1 Aljaber Ophthalmology and Otolaryngology Hospital, Otolaryngology Department, Ministry of Health, Ahsa, Saudi Arabia

2 King Abdullah Ear Specialist Center (KAESC), College of Medicine, King Saud University Medical City (KSUMC), King Saud University, Riyadh, Saudi Arabia

3 Research Department, MED-EL GmbH, Riyadh, Saudi Arabia

*Address all correspondence to: isra.aljazeera@gmail.com

IntechOpen

© 2023 The Author(s). Licensee IntechOpen. This chapter is distributed under the terms of the Creative Commons Attribution License (<http://creativecommons.org/licenses/by/3.0>), which permits unrestricted use, distribution, and reproduction in any medium, provided the original work is properly cited. 

References

- [1] Clark WW, Ohlemiller KK. *Anatomy and Physiology of Hearing for Audiologists*. New York: Thomson Delmar Learning, Singular; 2008
- [2] Olson ES, Duifhuis H, Steele CR. Von Békésy and cochlear mechanics. *Hearing Research*. 2012;**293**(1–2):31–43
- [3] Manley GA, Narins PM, Fay RR. Experiments in comparative hearing: Georg von Békésy and beyond. *Hearing Research*. 2012;**293**(1–2):44–50
- [4] Békésy G. Concerning the pleasures of observing, and the mechanics of the inner ear. Nobel Lect 1961
- [5] Kim J, Koo M. Mass and stiffness impact on the middle ear and the cochlear partition. *Journal of Audiology and Otology*. 2015;**19**(12):1–6. Available from: <https://www.ncbi.nlm.nih.gov/pmc/articles/PMC4491943/pdf/jao-19-1.pdf>
- [6] Greenwood DD. A cochlear frequency-position function for several species—29 years later. *The Journal of the Acoustical Society of America*. 2021;**87**(6):2592–2605. Available from: <https://pubmed.ncbi.nlm.nih.gov/2373794/>
- [7] Elfarnawany M, Alam SR, Rohani SA, Zhu N, Agrawal SK, Ladak HM. Micro-CT versus synchrotron radiation phase contrast imaging of human cochlea. *Journal of Microscopy*. 2016;**265**(3):349–357
- [8] Braun K, Böhnke F, Stark T. Three-dimensional representation of the human cochlea using micro-computed tomography data: Presenting an anatomical model for further numerical calculations. *Acta Oto-Laryngologica*. 2012;**132**(6):603–613
- [9] Hilding AC. Studies on the Otic labyrinth. *Annals of Otology, Rhinology & Laryngology*. 1955;**64**(1):278–290
- [10] Alexiades G, Dhanasingh A, Jolly C. Method to estimate the complete and two-turn Cochlear duct length. *Otology & Neurotology*. 2015;**36**(5):904–907
- [11] Erixon E, Rask-Andersen H. How to predict cochlear length before cochlear implantation surgery. *Acta Oto-Laryngologica*. 2013;**133**(12):1258–1265
- [12] Koch RW, Elfarnawany M, Zhu N, Ladak HM, Agrawal SK. Evaluation of Cochlear duct length computations using synchrotron radiation phase-contrast imaging. *Otology & Neurotology*. 2017;**38**(6):e92–e99
- [13] Helpard L, Li H, Rask-Andersen H, Ladak HM, Agrawal SK. Characterization of the human helicotrema: implications for cochlear duct length and frequency mapping. *Journal of Otolaryngology - Head & Neck Surgery*. 2020;**49**:6
- [14] Li PMMC, Wang H, Northrop C, Merchant SN, Nadol JB. Anatomy of the round window and hook region of the cochlea with implications for Cochlear implantation and other Endocochlear surgical procedures. *Otology & Neurotology*. 2007;**28**(5):641–648
- [15] Stidham KR, Rober JB. Cochlear hook anatomy: Evaluation of the spatial relationship of the basal Cochlear duct to middle ear landmarks. *Acta Oto-Laryngologica*. 1999;**119**(7):773–777
- [16] Helpard L, Li H, Rohani SA, Rask-Andersen H, Ladak HM, Agrawal S. Three-dimensional modeling and measurement of the human Cochlear hook region: Considerations for tonotopic mapping. *Otology & Neurotology*. 2021;**42**(6):e658–e665
- [17] JHE C, Gonzalez DL, Piro O. Pitch perception: A dynamical-systems

- perspective. Proceedings of the National Academy of Sciences. 2001;**98**(9): 4855-4859. Available from: http://www.iact.ugr-csic.es/personal/julyan_ca_rtwright/PDFs/37_2001_PNAS.pdf
- [18] Oxenham AJ, Micheyl C, Keebler MV, Loper A, Santurette S. Pitch perception beyond the traditional existence region of pitch. Proceedings of the National Academy of Sciences. 2011; **108**(18):7629-7634. Available from: <https://www.pnas.org/content/pnas/108/18/7629.full.pdf>
- [19] Litvak L, Delgutte B, Eddington D. Auditory nerve fiber responses to electric stimulation: Modulated and unmodulated pulse trains. The Journal of the Acoustical Society of America. 2001; **110**(1):368-379
- [20] Dynes SBC, Delgutte B. Phase-locking of auditory-nerve discharges to sinusoidal electric stimulation of the cochlea. Hearing Research. 1992;**58**(1): 79-90
- [21] Shannon RV. Temporal modulation transfer functions in patients with cochlear implants. The Journal of the Acoustical Society of America. 1992; **91**(4):2156-2164
- [22] Zeng F-G. Temporal pitch in electric hearing. Hearing Research. 2002;**174**(1-2):101-106
- [23] Bacon S, Fay RR. Compression: From Cochlea to Cochlear Implants. 2004th Edition. Springer Handbook of Auditory Research, Springer Science & Business Media; 2006
- [24] Semal C, Demany L. The upper limit of “musical” pitch. Music Perception. 1990;**8**(2):165-175
- [25] Attneave F, Olson RK. Pitch as a medium: A new approach to psychophysical scaling. The American Journal of Psychology. 1971;**84**(2):147
- [26] Burns EM, Feth LL. High-frequency pitch perception. The Journal of the Acoustical Society of America. 1983;**73**(S1):S44-S44
- [27] Langers DRM, van Dijk P. Mapping the tonotopic Organization in Human Auditory Cortex with minimally salient acoustic stimulation. Cerebral Cortex. 2011;**22**(9):2024-2038
- [28] Woods DL, Stecker GC, Rinne T, Herron TJ, Cate AD, Yund EW, et al. Functional maps of human auditory cortex: Effects of acoustic features and attention. PLoS ONE. 2009;**4**(4):e5183
- [29] Talavage TM, Sereno MI, Melcher JR, Ledden PJ, Rosen BR, Dale AM. Tonotopic organization in human auditory cortex revealed by progressions of frequency sensitivity. Journal of Neurophysiology. 2004;**91**(3): 1282-1296
- [30] Da Costa S, van der Zwaag W, Marques JP, Frackowiak RSJ, Clarke S, Saenz M. Human primary auditory cortex follows the shape of Heschl’s gyrus. Journal of Neuroscience. 2011; **31**(40):14067-14075
- [31] Griffiths TD, Hall DA. Mapping pitch representation in neural ensembles with fMRI. The Journal of Neuroscience. 2012;**32**(39):13343-13347. Available from: <https://www.ncbi.nlm.nih.gov/pmc/articles/PMC6621372/>
- [32] Stakhovskaya O, Sridhar D, Bonham BH, Leake PA. Frequency map for the human Cochlear spiral ganglion: Implications for Cochlear implants. Journal of the Association for Research in Otolaryngology. 2007;**8**(2):220-233
- [33] Zahara D, Dewi RD, Aboet A, Putranto FM, Lubis ND, Ashar T.

Variations in Cochlear size of Cochlear implant candidates. *International Archives of Otorhinolaryngology*. 2018; **23**(02):184-190

[34] Alshalan A, Abdelsamad Y, Assiri M, Alsanosi A. Cochlear implantation: The variation in Cochlear height. *Ear, Nose & Throat Journal*. 2022;**17**:0145

[35] Khurayzi T, Almuhawwas F, Sanosi A. Direct measurement of cochlear parameters for automatic calculation of the cochlear duct length. *Annals of Saudi Medicine*. 2020;**40**(3):212-218

[36] Helpard L, Li H, Rohani SA, Zhu N, Rask-Andersen H, Agrawal S, et al. An approach for individualized Cochlear frequency mapping determined from 3D synchrotron radiation phase-contrast imaging. *IEEE Transactions on Biomedical Engineering*. 2021;**68**(12): 3602-3611

[37] Dhanasingh A, Jolly C. An overview of cochlear implant electrode array designs. *Hearing Research*. 2017;**356**: 93-103

[38] Grover M, Sharma S, Singh SN, Kataria T, Lakhawat RS, Sharma MP. Measuring cochlear duct length in Asian population: Worth giving a thought! *European Archives of Oto-Rhino-Laryngology*. 2018;**275**(3):725-728

[39] Alanazi A, Alzhrani F. Comparison of cochlear duct length between the Saudi and non-Saudi populations. *Annals of Saudi Medicine*. 2018;**38**(2):125-129

[40] Canfarotta MW, O'Connell BP, Buss E, Pillsbury HC, Brown KD, Dillon MT. Influence of age at Cochlear implantation and frequency-to-place mismatch on early speech recognition in adults. *Otolaryngology-Head and Neck Surgery*. 2020;**162**(6):926-932

[41] Canfarotta MW, Dillon MT, Brown KD, Pillsbury HC, Dedmon MM, O'Connell BP. Insertion depth and Cochlear implant speech recognition outcomes: A comparative study of 28- and 31.5-mm Lateral Wall arrays. *Otology & Neurotology*. 2021;**43**(2): 183-189

[42] Boyd PJ. Potential benefits from deeply inserted Cochlear implant electrodes. *Ear and Hearing*. 2011;**32**(4): 411-427

[43] Hamzavi J, Arnoldner C. Effect of deep insertion of the cochlear implant electrode array on pitch estimation and speech perception. *Acta Oto-Laryngologica*. 2006;**25**:1-1

[44] Lee F-P, Hsu H-T, Lin Y-S, Hung S-C. Effects of the electrode location on tonal discrimination and speech perception of mandarin-speaking patients with a cochlear implant. *The Laryngoscope*. 2012;**122**(6):1366-1378

[45] Gani M, Valentini G, Sigrist A, Kós M-I, Boëx C. Implications of deep electrode insertion on Cochlear implant fitting. *Journal of the Association for Research in Otolaryngology*. 2007;**8**(1): 69-83

[46] van Besouw RM, Forrester L, Crowe ND, Rowan D. Simulating the effect of interaural mismatch in the insertion depth of bilateral cochlear implants on speech perception. *The Journal of the Acoustical Society of America*. 2013;**134**(2):1348-1357

[47] Buchman CA, Dillon MT, King ER, Adunka MC, Adunka OF, Pillsbury HC. Influence of Cochlear implant insertion depth on performance. *Otology & Neurotology*. 2014;**35**(10):1773-1779

[48] Canfarotta MW, Dillon MT, Buchman CA, Buss E, O'Connell BP,

Rooth MA, et al. Long-term influence of electrode Array length on speech recognition in Cochlear implant users. *The Laryngoscope*. 2020;**131**(4):892-897

[49] Zhou X, Li H, Galvin JJ, Fu Q-J, Yuan W. Effects of insertion depth on spatial speech perception in noise for simulations of cochlear implants and single-sided deafness. *International Journal of Audiology*. 2016;**56**(sup2): S41-S48

[50] Dincer D'Alessandro H, Ballantyne D, Boyle PJ, De Seta E, DeVincentiis M, Mancini P. Temporal fine structure processing, pitch, and speech perception in adult Cochlear implant recipients. *Ear and Hearing*. 2018;**39**(4):679-686

IntechOpen